
Use of PSInSAR data to map highly compressible soil layers

C. DEL VENTISETTE¹ L. SOLARI¹ F. RASPINI¹ A. CIAMPALINI¹ F. DI TRAGLIA¹ M. MOSCATELLI²
A. PAGLIAROLI² S. MORETTI¹

¹Department of Earth Sciences, University of Firenze
Via La Pira 4, 50121 Firenze, Italy

²CNR-IGAG, Institute of Environmental Geology and Geoengineering
Area della Ricerca di Roma 1. Montelibretti, via Salaria km 29,300, 00015 Monterotondo Stazione, Roma, Italy

| A B S T R A C T |

A new approach to the use of Persistent Scatterers (PS) Interferometry data in the reconstruction of the extension of compressible geological bodies is presented. The methodology was applied in the test area of the Tiber River delta (Italy), characterized by the presence of two large marshy zones, known as the Maccarese and Ostia Antica ponds. PSInSAR™ data, derived from ERS1/2, ENVISAT and RADARSAT-1 images, and spanning a time interval between 1992 and 2006 were used to verify the possibility to reconstruct the spatial distribution of the peat levels inside the Maccarese and Ostia Antica ponds. Borehole information was analyzed to calibrate the InSAR data and the deformation rates were used to hypothesize the presence of a thick compressible layer where geological information is lacking. Variations in deformation rates registered by the single PS were assumed to be representative of a variation in the stratigraphic asset. The obtained results demonstrate that this approach could be satisfactorily used to investigate wide areas in a short time, reducing the number of boreholes to drill, and it could be a complementary technique to obtain information about the 2D geometry of specific geological levels.

KEYWORDS | InSAR. PS analysis. Surface deformation analysis. 2D stratigraphic reconstruction. Tiber Delta. Peat.

INTRODUCTION

Mapping spatial distribution of clay and peat levels represent the starting point in many Holocene geology studies, from basin dynamic reconstructions to land subsidence hazard evaluation. Generally, mapping is based on geological field survey, often integrated with high resolution seismic lines analysis, and on the interpretation of the lithological description of boreholes. These approaches, despite allowing a high accuracy, require a large number of available data or the realization of new wells with economic and time loss.

Starting from the assumption that clay and peat levels are compressible layers, in this paper we propose a new procedure for mapping compressible subsurface layers based on the induced surface deformation detected by Synthetic Aperture Radar (SAR) interferometry. SAR interferometry (InSAR) technique can detect ground deformation by recording the satellite-to-ground signal phase difference between two satellite data acquisitions (Massonnet and Feigl, 1998). Advanced Differential Interferometric Synthetic Aperture Radar (A-DInSAR) has been confirmed as an effective technique for the mapping and study of ground deformation dynamics (both spatial and temporal) related to slow landslides (*e.g.*, Hilley *et*

al., 2004; Farina *et al.*, 2006; Cigna *et al.*, 2010, 2011; 2012, 2013; Bianchini *et al.*, 2012, 2013; Ciampalini *et al.*, 2012; Tofani *et al.*, 2014; Del Ventisette *et al.*, 2014), tectonic motions and tectonic activity (*e.g.*, Colesanti *et al.*, 2003; Bürgmann *et al.*, 2006; Massironi *et al.*, 2009; Perrone *et al.*, 2013), land subsidence (*e.g.*, Canuti *et al.*, 2005; Stramondo *et al.*, 2008; Osmanoglu *et al.*, 2011; Del Ventisette *et al.*, 2013), and volcanic activity (*e.g.*, Salvi *et al.*, 2004; Tizzani *et al.*, 2007).

This new A-DInSAR application allows to map subsurface compressible geological layers identifying ground deformation (related to the compaction of the sedimentary body) within an area where no other causes are identified to explain the recorded subsidence. This application allows the 2D reconstruction of the geometry of shallow sedimentary layers characterized by high compressibility that can induce ground subsidence. We therefore suggest an application of the PS technique, in support of stratigraphic reconstructions usually derived from conventional geological survey, seismic line interpretation and boreholes data. The selected test site is located in the Tiber Delta (Italy), where in Maccarese and Ostia Antica area two ancient coastal ponds developed about 4500yrs ago and are completely filled today. The stratigraphy and geometry of the Tiber Delta is well known mainly through the interpretation of well data and seismic lines, used to implement delta evolution models (Belluomini *et al.*, 1986; Bellotti *et al.*, 1987, 1995, 2007; Giraudi, 2004). The geological reconstruction of a compressible geological body has been used to validate the results obtained from A-DInSAR data interpretation.

Results demonstrate that this approach could be suitable to investigate wide areas in a short time, drilling only few wells and could be a complementary technique to obtain information about the 2D geometry of specific geological levels providing better spatial resolution and comparable accuracy.

GEOLOGICAL BACKGROUND OF THE TIBER DELTA

The deltaic system of the Tiber River (Italy) is located few kilometers southwest of Rome, with an extension of about 40km parallel to the coast. The emerged part is 150km² wide, whereas the submerged sector is about 500km² with a maximum sedimentary body's thickness slightly greater than 80m (Capelli *et al.*, 2007). The Tiber Delta is a wave dominated delta (Bellotti *et al.*, 2007; 2011; Milli *et al.*, 2013), and it consists of an outer delta (from 0 to 7m a.s.l.) mainly formed by beach ridges and dunes, and an inner delta containing depressions (until 1.2m below sea level) of drained marshes (Fig. 1). These today reclaimed marshy areas correspond to the ponds (known as "stagni") of Maccarese and Ostia.

The evolution of the Tiber Delta can be reconstructed since the Early Pleistocene, when the area was completely submerged (Bellotti *et al.*, 2007; Milli *et al.*, 2013), as testified by the presence of clay and clay-mud sediments with interbedded levels of fine sands deposited in a shelf environment. The top of these deposits lies between 25 and 80m in depth. During the Middle Pleistocene the shelf environment was replaced by a shoreface to backshore and lagoon environment. This succession (Ponte Galeria Formation) is exposed in the northern sector of the study area (Pleistocene hills in Fig. 1), whereas it is buried southward and its top span between *ca.* 10 and 30m in depth. On the aforementioned deposits lie in unconformity, marked by a well developed erosive surface, the Upper Pleistocene–Holocene Tiber Delta sediments. The evolution of the Tiber Delta can be summarized in five steps (Milli *et al.*, 2013 see Figure 1).

The compressible layers of the Tiber Delta were deposited during the Transgressive and Highstand System Tracts (Table 1), mainly starting 13Kyr BP. At that time, a barrier-island system and a lagoonal basin developed in NW-SE direction, and the Tiber River began to form a bay-head delta (Milli *et al.*, 2013). The lagoonal basin constituted the prodelta region of the bay-head delta; peat and organic rich deposits are typical of this environment. The final sedimentation phase of the Transgressive System Tract (TST) in the lagoon is characterized by the deposition of a thick (2 to 7 meters), continuous peat layer (6–5Kyr BP; Milli *et al.*, 2013). The formation of the peat layer coincides with the closure of the TST, in correspondence of the maximum flooding surface (mfs in Fig. 1); this surface is placed at the top of organic rich deposits with peat layers (Raspa *et al.*, 2008).

6–5Kyr BP the lagoon was transformed into two marshy coastal ponds, the Maccarese pond to the north and the Ostia pond to the south. The evolution of the

TABLE 1. Upper Pleistocene-Holocene evolutionary stages of the Tiber delta plain (data from Milli *et al.*, 2013)

Time before present	Phase	Present day position	Depositional system
120 to 14 Kyr BP	Lowstand System Tracts	-80 m to -50 m above sea level (a.s.l.)	Fluvial
14 to 5-6 Kyr BP	Transgressive System Tract	-50 m to a depth ranging between -25 and -5 m a.s.l.	Fluvial-bay-head deltaic system, coastal barrier-lagoon system, transition to shelf system
5-6 to 2,7 Kyr BP	Highstand System Tract-first phase	-40 m a.s.l. to approx. sea level	Coastal barrier-lagoon system
2,7 to 1,9 Kyr BP	Highstand System Tract-second phase	approx. sea level	Coastal barrier-lagoon system
1,9 Kyr BP to present day	Highstand System Tract-third phase	approx. sea level	Coastal barrier-lagoon system

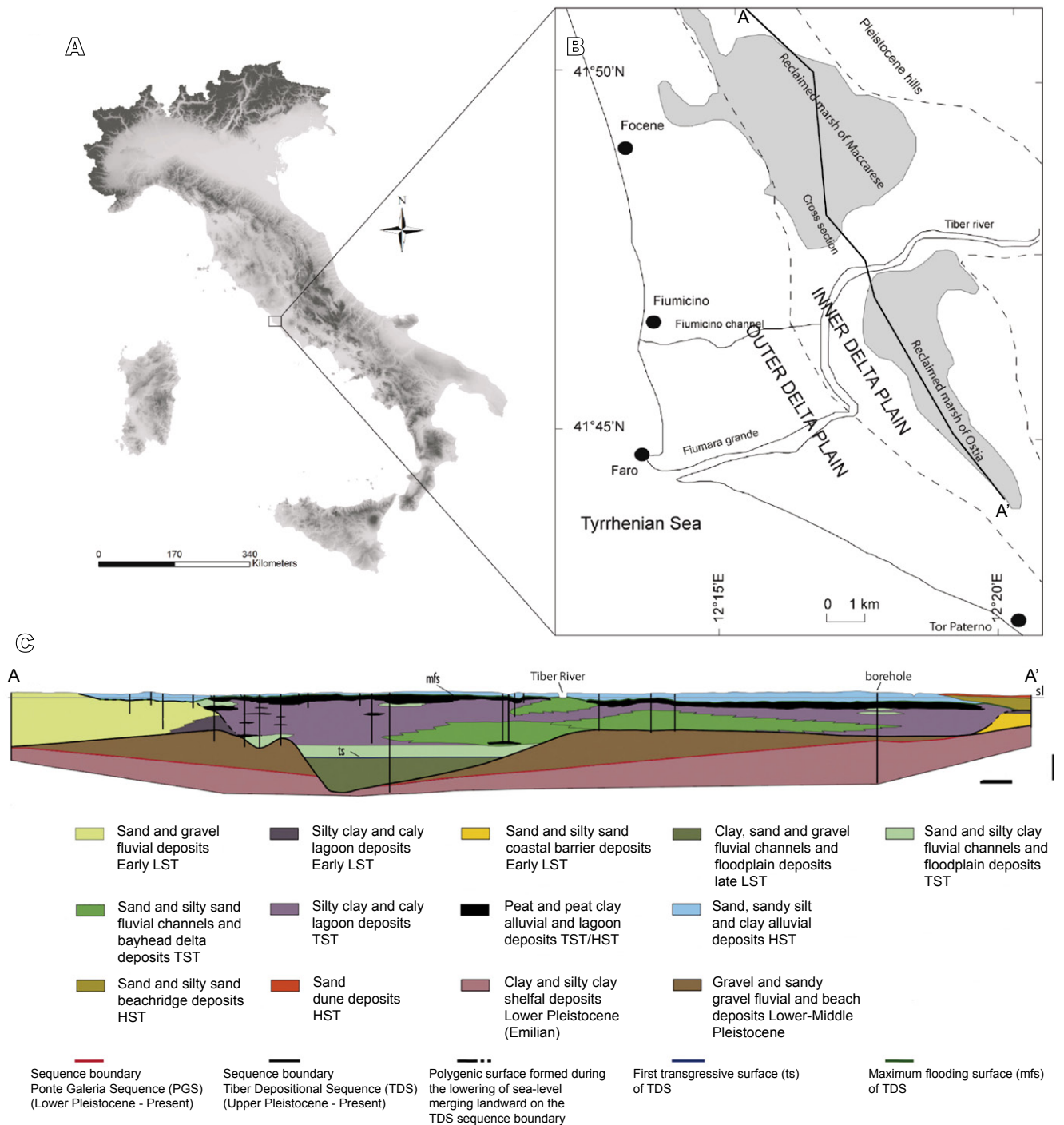


FIGURE 1. Location of the study area on 20m DEM. A); Tiber Delta domains (redrawn after Bellotti *et al.*, 2007) B); cross section of the delta plain (redrawn after Milli *et al.*, 2013). The track of the cross section c) is shown in b). In the cross section C) the peat layers that characterize the Maccarese and Ostia ponds are shown.

Maccarese and Ostia ponds highlights the presence of two main evolutionary stages; the first (before the tenth-ninth centuries BC), when the ponds were not connected with the sea and were fed by fresh water (rain, groundwater, local streams), the second, when the sandy barrier collapsed (from the fifteenth century AD), the sea water penetrated the marsh thanks to inlet channels and the water became brackish (Giraudi, 2011).

The sedimentary section of the Maccarese area can be divided in several units (Giraudi, 2011). The stratigraphically lower part is made of lagoonal grey–light blue clays, overlies by the oligoaline water deposits mainly composed of clays, peaty silts and peats with palustrine malacofauna. Upwards the section continues with brackish sediments characterized by the presence of grey silts and clayey silts with brackish water malacofauna and rare sandy gravel levels deposited by flood events of the Tiber River. The uppermost part testifies the return of the marsh environment, highlighted by the deposition of yellowish–gray silts with oligoaline malacofauna.

The Maccarese and Ostia ponds were reclaimed, starting from 1884, to obtain new agricultural and building areas. The reclamation was carried out with a network of pumping plants (Amenduni, 1884) which raised the water draining it into the sea through artificial channels. The process ended in the first part of the 1900s.

This stratigraphic framework is the result of the Delta evolution over the past 20,000 years. The Holocene landscape evolution of the study area, characterized by a substantial tectonic stability, was controlled by the rates of postglacial sea-level rise and fluvial input. The Tiber Delta is affected by a slight subsidence of less than 0.6mm/y (Amorosi and Milli, 2001) mainly due to the deformation of a peat layer (Giraudi, 2011).

METHODS AND DATA

This paper proposes a new application of the radar interferometry to reconstruct the extension of compressible layers at depth, assuming the ground deformation rate to be essentially related to the change in local stratigraphy and in particular to the thickness of highly compressible layers. The applied methodology (Fig. 2) is based on a ground deformation analysis based on PSInSAR information to reconstruct the extension of subsidence area. This procedure was tested into two selected sites: the Maccarese and the Ostia ponds.

In order to reconstruct the extent and rate of the ground subsidence phenomena and to investigate the past evolution of the ground movements affecting the Tiber deltaic area, a PSI analysis has been carried out, processing three stacks of C-band SAR images acquired by ERS 1/2, ENVISAT and RADARSAT-1 satellites in descending orbit, spanning a time interval between 1992 and 2006 acquired in the framework of ESA-GMES TerraFirma Extension project (for this reason the analysed radar images are limited to 2006).

The three datasets have been processed with PSInSAR technique (Ferretti *et al.*, 2000; 2001), the first of the many techniques, grouped under the family name Persistent Scatterer Interferometry (PSI), specifically implemented for the processing of multi-temporal radar imagery. Specifically, PSInSAR is a multi-interferometric processing technique relying on the phase signal analysis of a network of coherent radar targets (Permanent Scatterer, PS). The main idea underpinning this technique is the identification, throughout every image of the observation time period, of pixels that exhibit stable amplitude and coherent signal phase. Statistical analysis of backscattered phase signal allows estimating occurred displacement, acquisition by acquisition, by distinguishing the deformation due to ground motions from the contributions related to atmosphere, topography and noise.

Having subtracted the topographic information (through the use of InSAR DEM) and having removed the atmospheric artifacts superimposed on the signal of interest, the remaining interferometric data are displacement value and noise. The latter can be most likely considered negligible within the processing chain of the PSInSAR technique, since, by definition, each identified PS is a point-like target characterized by high signal to noise ratio. Once all the spurious components are removed, ground deformation for each radar target is retrieved.

All measurements are calculated along the satellite LOS (Line of Sight) and referred temporally and spatially to a unique reference image and to a pre-selected reference

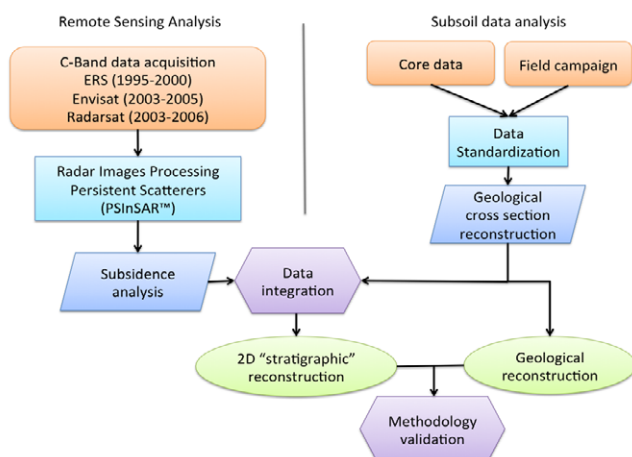


FIGURE 2. Proposed workflow to use PSInSAR data to support geological interpretation of sub-surface data analysis.

point in the PS network. The reference points of the stacks –whose proper selection during the processing activity is of crucial importance to avoid the retrieval of unreal pattern of deformation– are located in the low energy hilly areas bordering the urban fabric of Rome. Apart from the phase stability throughout the dataset, the reference point is chosen in an area assumed devoid of ground motions. The

chosen reference points are located on sandy formations or on massive volcanic deposits, safely considered as stable, most likely to be unaffected by local scale deformation processes related to hydrogeological factors.

By examining large stacks of SAR images (higher their number, more accurate the results), many differential

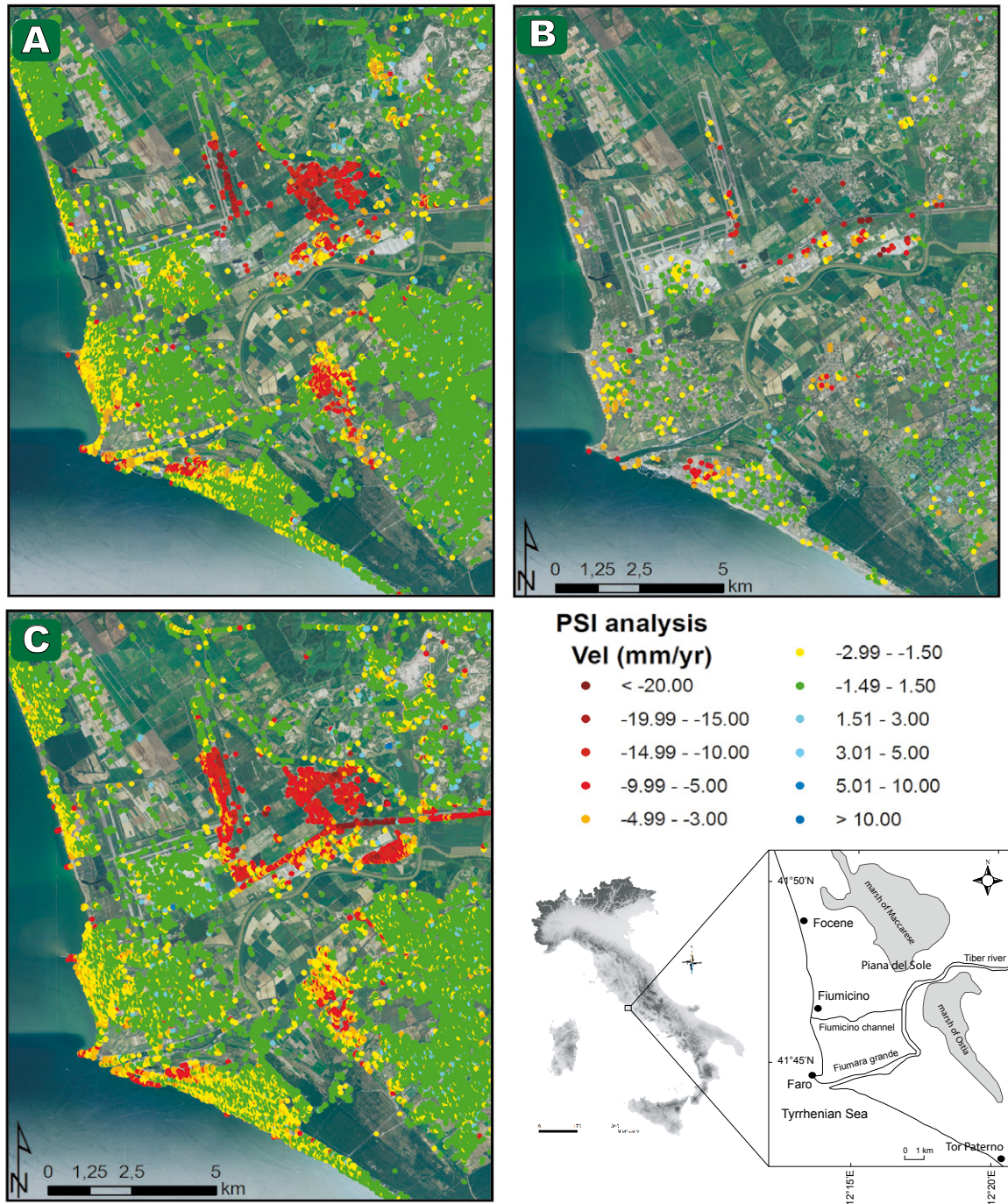


FIGURE 3. Interferometric dataset used in this work: A) ERS; B) ENVISAT and C) RADARSAT-1.

interferograms are generated by selecting one of the scenes as a master to which the other scenes become slaves. All available images of the data stack are focused and co-registered on the reference sampling grid of a single master acquisition. It has been proved (Kampes, 2006) that the stack coherence is larger when the master is selected centrally in time. On the other hand coherence decreases when the master does not lie centrally with regard to the temporal, geometrical and Doppler baseline.

The availability of three different data stacks (founded by ESA-GMES TerraFirma Extension project) has allowed the reconstruction of the deformation pattern for a 15 years-long period, spanning time interval between 1992 and 2006 (Fig. 3). Details of satellite SAR imagery, employed for the reconstruction of temporal evolution and spatial patterns of the subsidence, are reported in Table 2. For each dataset, the master image has been chosen centrally, to maximize the coherence of the computed interferograms.

Sub-surface stratigraphy in the Tiber Delta plain was reconstructed on the basis of a large georeferenced database, provided by the CNR-IGAG developed in the framework of URBISIT project (funded by Italian Department of Civil Protection, DPC), consisting of approximately 300 boreholes (Fig. 4) of which 93 and 58 well logs for Maccarese and Ostia Antica test site, respectively. Well logs range in depth between 10 to 50m. The database provides, for each borehole, technical information (*i.e.* depth, elevation, date, geographic coordinates), the stratigraphy and several hydrogeological information (depth of the water table, conductivity, pH, transmissivity, storage coefficient).

Boreholes data were described in terms of mean grain size, texture, color, sedimentary structures and accessory materials. Compressibility sediments classification was based on their lithofacies and available geotechnical parameters. The classification led to the identification of 4 compressibility classes: 1) peat and decaying material, organic clays and clay with peaty levels; 2) inorganic clays, silty clays, clayey silts and silts; 3) silty sands,



FIGURE 4. Localisation of available boreholes collected in the URBISIT database.

sandy silts and fine to very fine sands; 4) medium to coarse sands, gravely sands, sandy gravels and gravels. The first two classes (*i.e.*, soft normally-consolidated organic or inorganic clays) are considered compressible, the remaining as incompressible.

Paleogeographic interpretation was based upon several key papers dealing with the evolution of the Tiber Delta plain (Bellotti *et al.*, 2007; Giraudi, 2011). The integration between the ground deformation velocity maps, obtained through PSInSAR data, and the subsurface geological data (Step “Data Integration” in Fig. 2) have been performed comparing the deformation rates profiles and the thickness of the peat level along the geological sections in both the Maccarese and Ostia areas. These profiles were produced using the punctual data of the PS velocity.

DATA ANALYSIS AND RESULTS

Maccarese pond

The PSI data distribution in the Maccarese area (Table 2; Fig. 3) shows large variability with a maximum density near the runways of the Leonardo Da Vinci International Airport and on the urbanized areas, and a minimum density in the agricultural area between the airport and Piana del Sole area. Ground deformation velocity maps highlight that ERS 1/2 (Fig. 5A) and RADARSAT-1 (Fig. 5C) are characterized by a high PS density, whereas ENVISAT (Fig. 5B) shows a very low PS density (due to the limited number of available images), not sufficient to understand the ground deformation phenomena that affect this area.

TABLE 2. Details of the SAR datasets processed in this study

Satellite	Time interval (# scenes)	Master image	Wide area: Tiber Delta		Maccarese area		Ostia area	
			Identified PS	PS density (PS/km ²)	Identified PS	PS density (PS/km ²)	Identified PS	PS density (PS/km ²)
ERS1/2	21/04/1992 -29/12/2000 (65)	26/07/1997	17105	51	2659	52	1435	68
ENVISAT	03/01/2003 -01/07/2005 (13)	23/01/2004	1404	4	156	3	113	5
RADARSAT1	15/03/2003 -18/11/2006 (49)	28/03/2005	18745	56	1480	30	1674	82

Despite the different time coverage, acquisition mode and PS density, ERS 1/2 and RADARSAT-1 datasets indicate a clear and unambiguous pattern of deformation. A zone, located in correspondence with the Piana del Sole and characterized by high deformations rate (up to 45mm/yr; value recorded in few points along the eastern part of the A91 highway), can be recognized (Fig. 5A, C). Within the RADARSAT-1 ground deformation map, the abrupt change in the average deformation rate, in the N/S-oriented runway of the international airport, is evident. Here the recorded velocities changes quickly from the stability range to more than -20mm/yr.

Moving from the delta area to the Pleistocene hills (from SE to NW; Fig. 5) an increase of deformation rate is observed. This trend is clearly visible along the A91 highway (where the deformation rate is more than -20mm/

yr). In correspondence with the Pleistocene hills the ground deformation velocities fall down again into the stability range (defined between -1.5 and +1.5mm/yr).

In the Maccarese/Piana del Sole area, boreholes are present only along the major highways and along the runway areas (Fig. 6). In this area (Fig. 7) a peaty organic level, with variable thickness, at a depth ranging between +4m a.s.l. (*e.g.* P9754, P9753) to -7m a.s.l. (*e.g.* P9807, P9762) is present. This organic layer represents the typical marshy sedimentation of the Maccarese pond (Bellotti *et al.*, 2007; Giraudi, 2011; Milli *et al.*, 2013). Other local peat levels are located at a depth of -10m a.s.l. and -15m a.s.l. in correspondence with boreholes P9750 and P9750 (profile AA', Fig.7). The peats extend with continuity for about 4–5km in north-south direction (*e.g.* P9739 and P18503) and about 5km in east-west direction (*e.g.* P9774

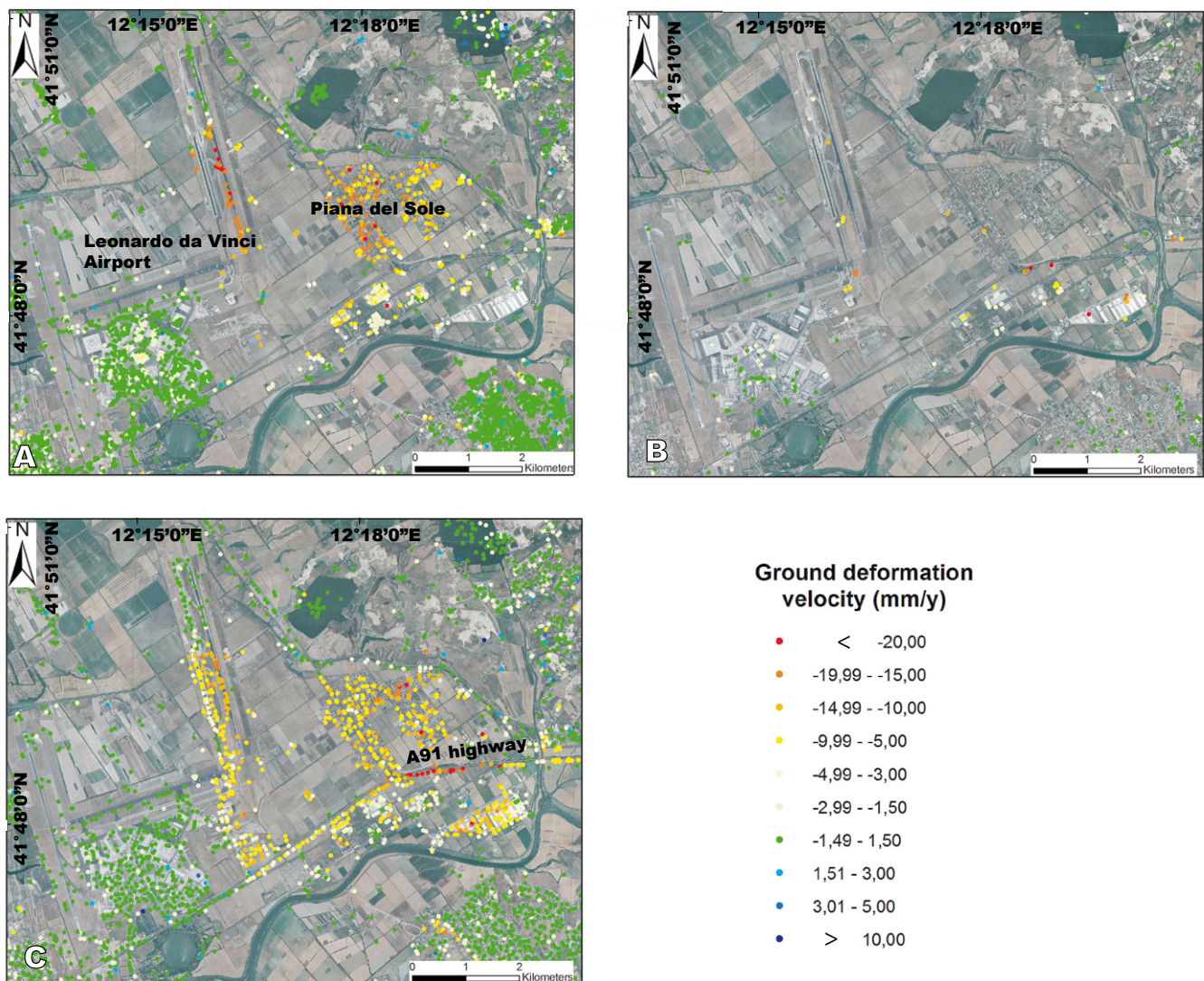


FIGURE 5. Ground deformation velocity maps in the area of Maccarese. A) ERS 1/2 (1992–2000); B) ENVISAT (2003–2005); C) RADARSAT-1 (2003–2006).

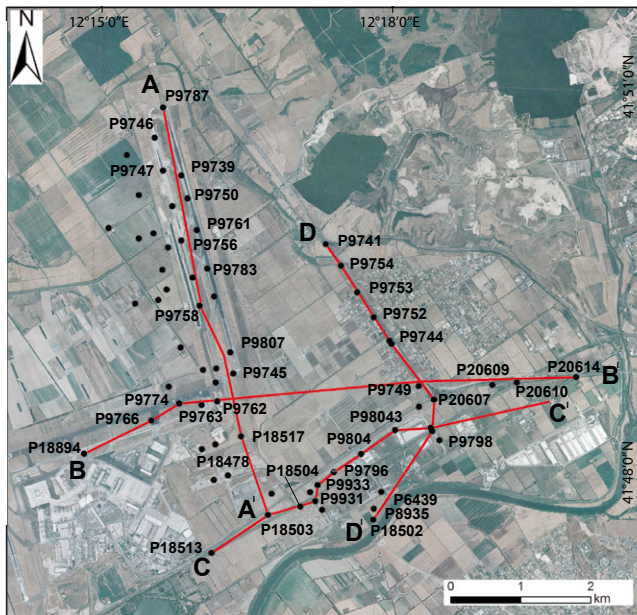


FIGURE 6. Location of the boreholes and the analyzed stratigraphic profiles in the Maccarese area.

and P20614). In the borehole P9749 (Figure 7) this level was not observed, probably due to a local difference in the ancient swamp morphology. The organic layer is bounded to the W–NW mainly by sandy sediments (classified as class 4 –P9774 and P9746) and to the E by layers of sandy silts (classified as class 3 –P20614). The class 4 deposits correspond to the Lowstand System Tract deposits of the Tiber Depositional Sequence described by Milli *et al.* (2013). The sediments classified as class 1 are not detected west of the airport runway area (P9774, P9776, P18494) and in the area near the Tiber River (P18502 and P9935) where they are replaced by fluvial sediments of the Tiber River. Also in the boreholes located along the A91 highway (*e.g.* P20614) and close to the eastern boundary of the pond, the peat layers thickness decreases. The class 2 is the most widespread in the subsurface of the studied area, and it is characterised by an extremely variable thickness, ranging between 10 (*e.g.* P9798) and 30m (*e.g.* P20614). A clear correlation between the observed deformation pattern and the geological features is observed: for instance, the abrupt change in the deformation rate along the NS runway of the airport corresponds to the transition from class 4 stiff sediments to 1–2 soft organic and inorganic clays. This aspect is investigated in more details in the following paragraphs.

Ostia Antica pond

In the Ostia Antica area the ERS frame has an average density of 68PS/km², ENVISAT 5PS/km² and RADARSAT-1 82PS/km² (Tab. 2; Fig. 3); in the north-western part of this area, the values of density decrease

quickly along the time-span given by the three successive datasets (Fig. 8).

Ostia Antica shows an elongated SE–NW oriented sector characterized by an average deformation rate between -4mm/yr to -15mm/yr; outside this zone the deformations decreases down into the stability range (Fig. 8). This behavior is similar to that observed in the Maccarese area, although the deformation rates registered here are lower. The direction of the area affected by ground deformation phenomena changes northward, where the orientation is SW–NE (Fig. 8). The change in orientation is already visible in ERS dataset and clearly showed in the RADARSAT dataset, which is characterized by a higher PS density. The north-eastern sector affected by subsidence shows deformation rates comparable with those in the main sector of the Ostia Antica pond (Fig. 8).

In the Ostia area, the density of the boreholes is lower with respect to the Maccarese area (Fig. 9), especially in the southern sector. The site is characterized by a peat layer identified in all the boreholes located at the central part of the area (*e.g.* P14276 and P18501). These deposits, classified as class 1, are observed at depths ranging between -2m (P14288) and -7m a.s.l (P14276) with a thickness varying between 1m (P14244 and P14264) and 5m (P14276). It represents the marshy sedimentation of the ancient pond of Ostia (Bellotti *et al.*, 2007).

Also in this case higher ground deformation rates (revealed by SAR images) are concentrated where highly compressible soil layers (class 1–2 sediments) are found: see section BB' in Figure 9, where the recorded deformation rate is up to 10mm/yr in association with an estimated compressible layers thickness of 8 meters (class 1–2 sediments). In comparison to the peaty layer of Maccarese, the compressible layer of the Ostia Antica pond turns out to be of minor extension and thickness; furthermore the clay level classified in class 2 below the organic level is less extended in depth (never more than 5m thick, *e.g.* P14276). Another substantial difference with the Maccarese area is the almost total absence of the sandy silt level (class 3, with the exception of P6456). This makes the stratigraphy less complex, consisting essentially, besides the -15m, of sands and gravel. This thickness of the class 4 level reaches 30m (P6462), suggesting that the Ostia pond was smaller and shallower than the one of Maccarese, probably because of the inherited morphology of the substratum (see Fig. 1).

DISCUSSION

The comparison between the deformation rate profile and the thickness of the peat layer in Maccarese area shows a good agreement: a general increase of the

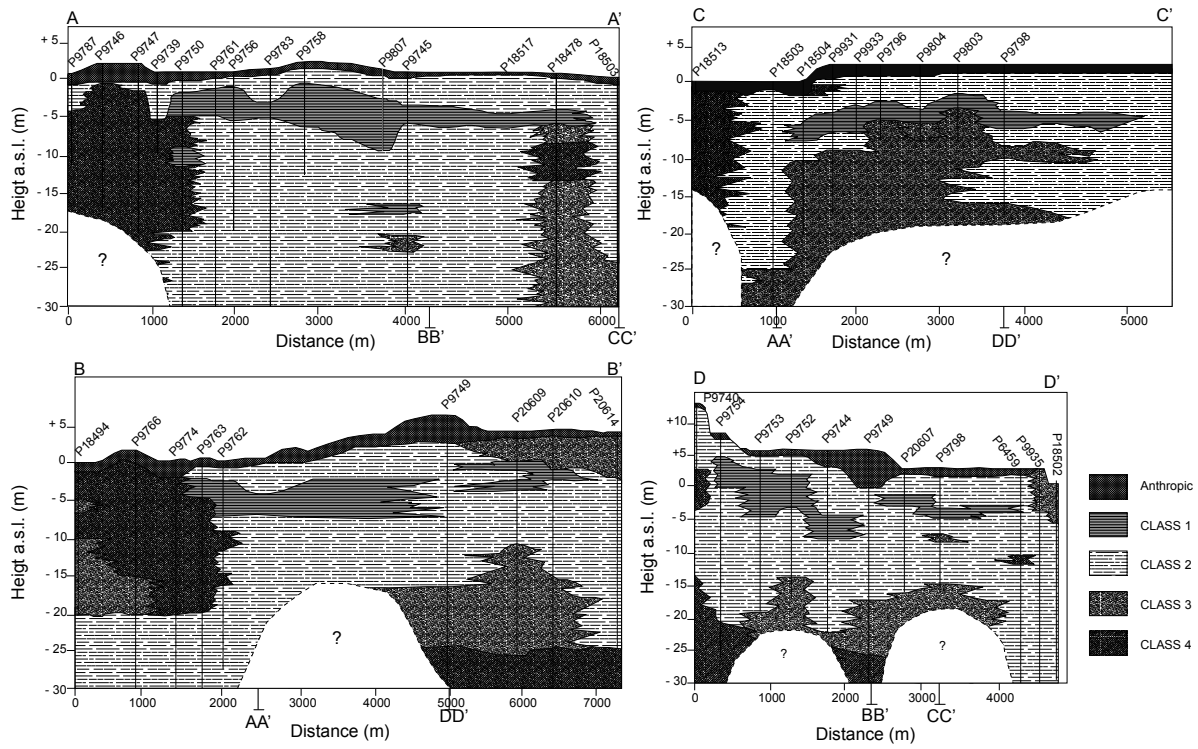


FIGURE 7. Reconstruction of the subsurface stratigraphic profiles in the Maccarese area.

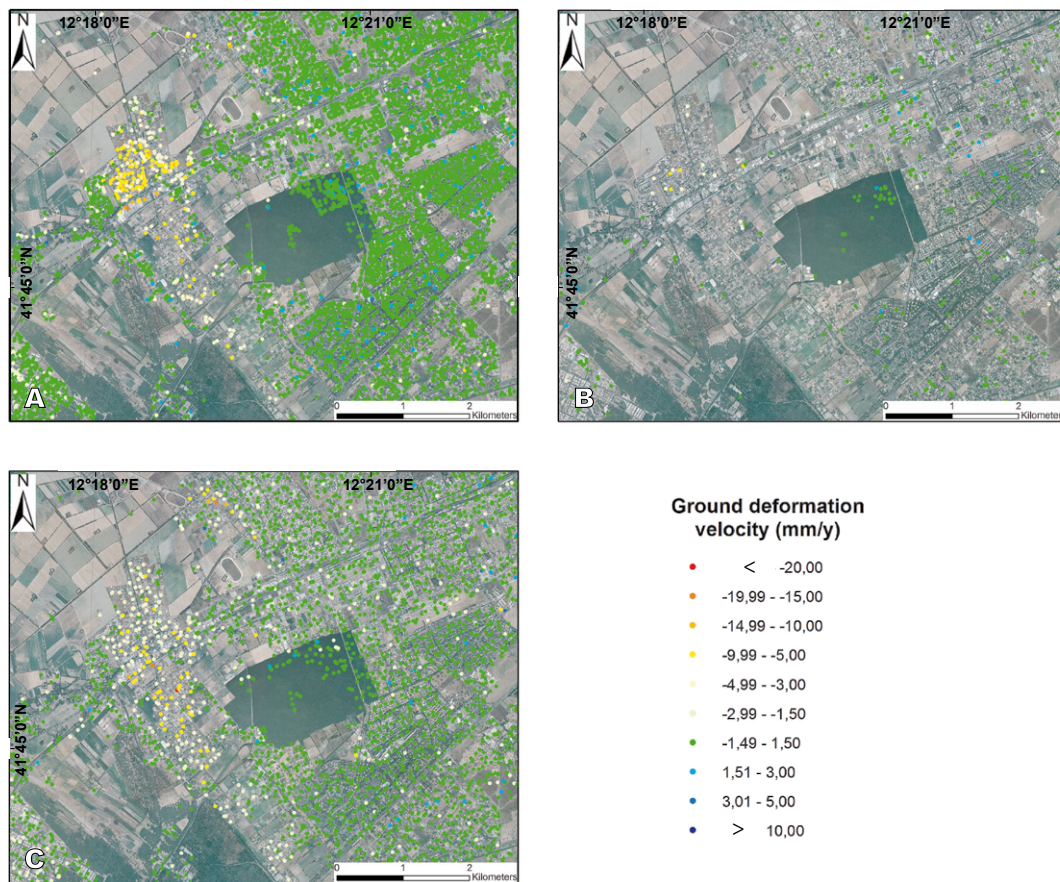


FIGURE 8. Ground deformation velocity maps in the area of Ostia. A) ERS 1/2 (1992–2000); B) ENVISAT (2003–2005); C) RADARSAT-1 (2003–2006).

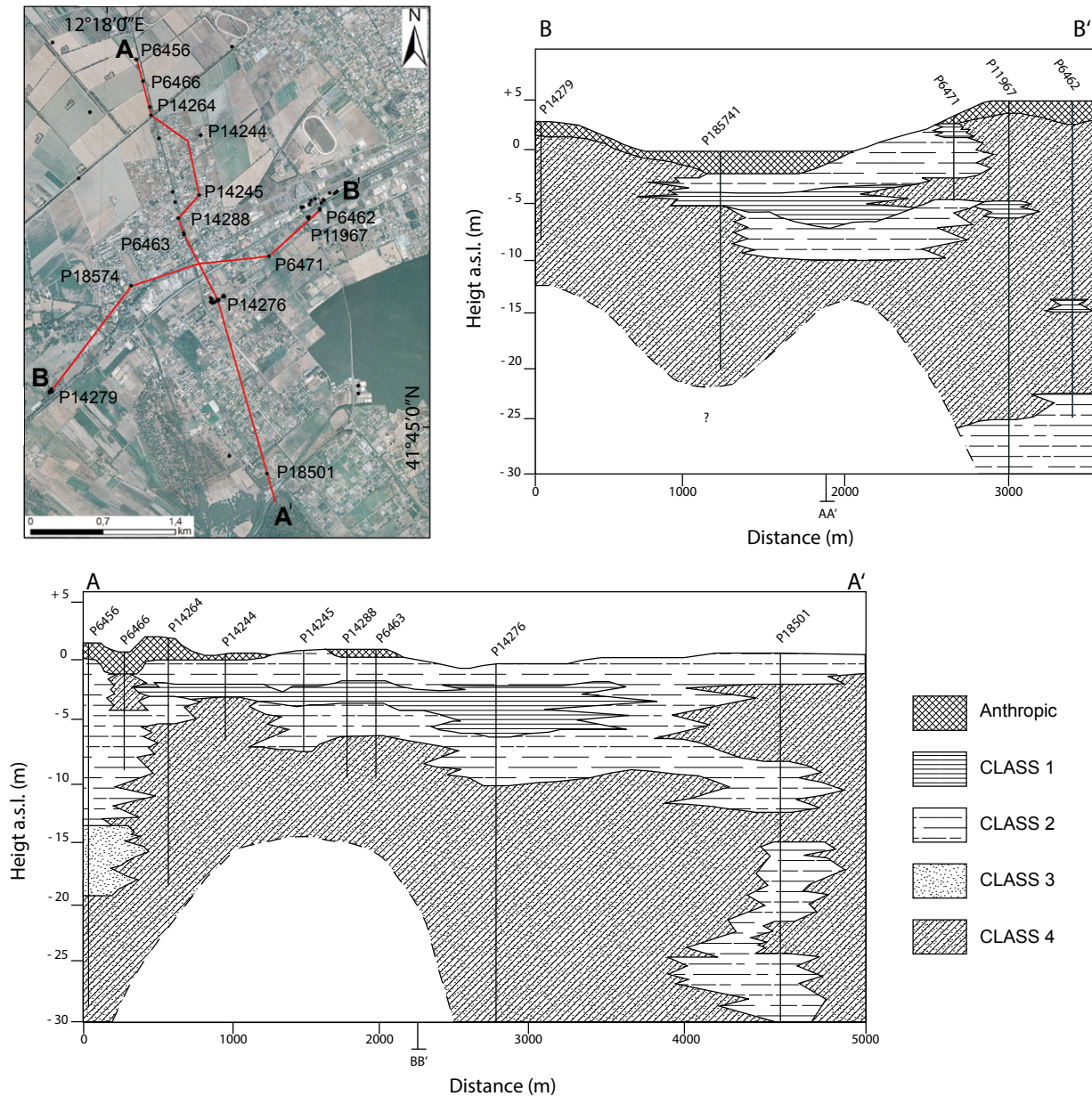


FIGURE 9. Used boreholes and geological cross-sections in the Ostia Antica area. The black dots with the identification code indicate the location of the boreholes.

ground deformation velocity values corresponds to an increase of the peat layer thicknesses, especially along the A–A' and D–D' geological sections (Fig. 10A, D). This behaviour is less marked along the B–B' profile (Fig. 10B). The minor order oscillations in the deformation profiles can be explained considering the lateral variation on the lithotypes. Also the thickness of sediments classified as class 2 (compressible layers) seem to affect the subsidence rate. This is evident in the western part of the C–C' section (Fig. 10C) where the ground deformation velocities show an abrupt increase in correspondence of the maximum thickness

(about 25m) of class 2 sediments. On the contrary, the presence of class 3 layers (sandy silts levels) smooth out the ground deformation rate, which tends to be stable in correspondence of the presence of this class in the subsurface.

Also in the Ostia area, the deformation rate profiles (Fig. 11A, B) show peaks, corresponding to the PS having the highest velocities, located in the central part of the pond where the maximum thickness of the peat level (class 1) is detected. In this area class 2 layers do not present significant thicknesses and class 3 sediments have not been

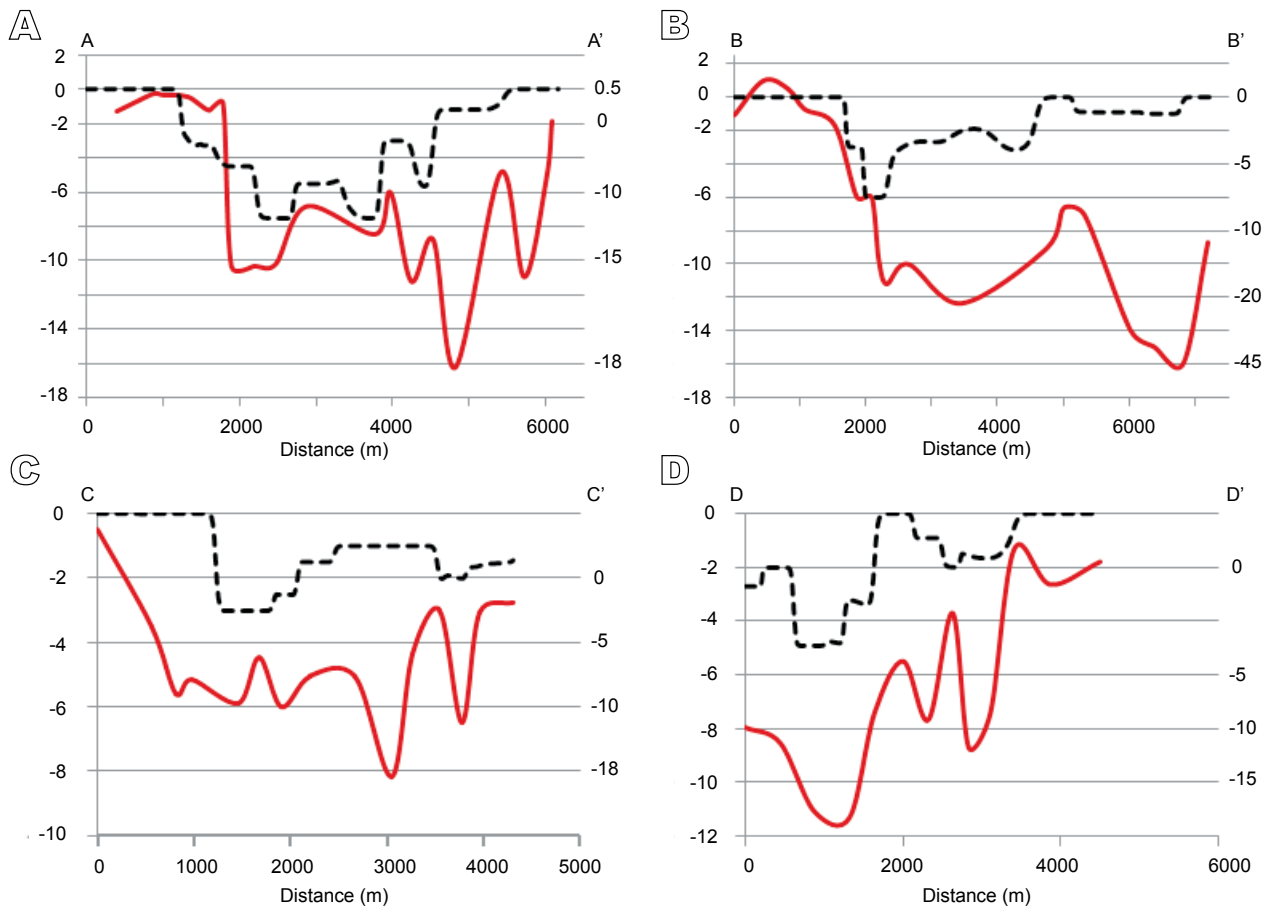


FIGURE 10. Variation of deformation rates along the four geological cross-sections in the Maccarese area (A–D). Left y-axis: thickness of the peat layers (in meters); right y-axis: mean PS velocity (in mm/y). The red line represents the profile based on the punctual PS velocity and the black dashed line represents the peaty horizon thickness.

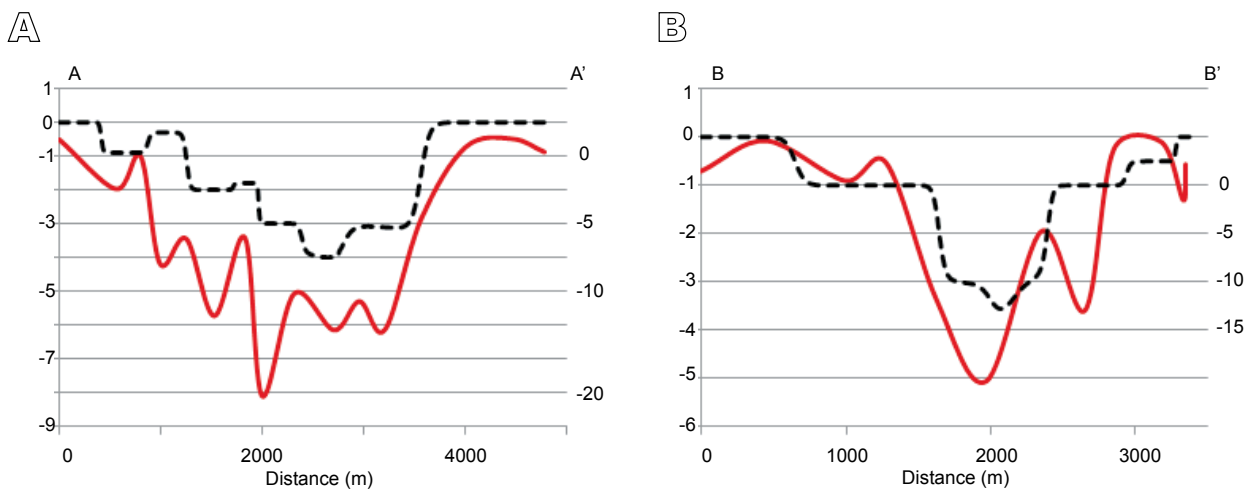


FIGURE 11. Deformation rate variation along the two geological cross-sections in the Ostia area (A–B). Left y-axis: thickness of the peat layers (in meters); right y-axis: mean PS velocity (in mm/y). The red line represents the profile based on the punctual PS file and the black dashed line represents the peaty horizon thickness.

recognized. The correlation between the thickness of the peaty layer and the ground deformation velocity is very promising.

From data analysis in Ostia area, it is pointed out that the occurrence of organic soft sediments is an important conditioning factor for subsidence. An attempt to establish a correlation factor between the ground deformation velocities and the thickness of the compressible layers has been performed in the Ostia Area using the RADARSAT-1 dataset which is characterized by the highest PS density. Here, the coefficient of determination (R^2) between the displacements retrieved by PSI data and the thickness of soft soils (class 1–2) is 0.81 (Fig. I, Electronic Appendix). The displacement magnitude and soft soil thickness are directly correlated. ERS1/2 and ENVISAT, due to few available images, are characterized by a lower density and do not allow an accurate assessment of this relationship. In the Maccarese area the R^2 coefficient is lower (equal to 0.4). This minor degree of correlation can be due to the wide presence of class 3 deposits which seems to attenuate the subsidence of the area.

The results show that there is a direct relationship between the presence and thickness of compressible layers and the deformation rates registered by the PS. Indeed, not only the presence of class 1 layer (organic clays) affects the registered deformation rates, but a crucial role is carried out by the thickness of class 2 layer (soft inorganic clays). A clear example is the right-side of the profile associated to the geological section B–B' (Fig. 10B). In fact, despite the decreasing thickness of the class 1 layer, the deformation rate trend is characterized by a constant descending curve; this is related to the presence of highly compressible class 2 layers. This is a case in which the presence of class 1 layers could not completely explain the recorded vertical displacements; the contemporaneous presence of class 1 and class 2 layers with heavy loads on the surface can better justify the deformations.

The mapping of the two studied ponds using the available subsurface data is affected by a generalized low density of boreholes (Fig. II). This issue is even more evident in the case of Ostia, where the detection and reconstruction of the peat layer (class 1) were performed using less than 25 boreholes. On the other hand, the spatial extension of the compressible layers, based on the PS data (Fig. III), was defined starting from the evidence that there is a clear lowering in the deformation rates registered out of the limit of the marshy zones (strong variation from -10/-15mm/y to less than -3mm/y). The importance of the boreholes density in subsurface stratigraphic reconstruction is highlighted by the comparison between Figures II and III. The good

correspondence between the contours in Figure IIA and Figure IIIA, thanks to the greater availability of boreholes, was not repeated in Figure IIB and Figure IIIB. When subsurface data are insufficient the PSInSAR technique can be useful for mapping compressible layers, given to the high density of scatterers.

In the central part of the Maccarese area there is a good agreement between the two boundaries (Fig. 12). On the contrary, significant differences are observed in the north-western and southern sectors. In particular, the southern sector inferred by the PS plus borehole data is more expanded towards the Tiber River. In the Ostia area a better agreement between the two perimeters is observed. In fact, excluding minor variations in the width of the pond, significant differences are only found in the southern sector.

CONCLUSIONS

According to the purpose of this work, the PSInSAR technique was coupled with the geological information of the available boreholes to map the extent of the peat layer in the Maccarese and Ostia Antica ponds. The obtained contours were compared with the perimeter of the two pond areas inferred in the available literature to appreciate the quality of this method.

In conclusion, the proposed methodology has permitted an accurate mapping of the areal distribution of the organic clay layers present in the Maccarese and Ostia ponds; this was possible thanks to the combined use of boreholes information and interferometric data. The PSInSAR data with their greater density of points have provided the possibility to hypothesize the areal distribution of the peat layer after the calibration on few boreholes. This approach is a useful tool to expand, at a relatively low cost and short time, a stratigraphic analysis of geological bodies with characteristics (*i.e.* high compressibility) that can be detected by the A-DINSAR technique. Moreover, the methodology could be applied to not well known or not easily accessible areas, where an extensive geognostic survey cannot be carried out.

ACKNOWLEDGMENTS

The ESA-GMES TerraFirma Extension project (www.terrafirma.eu.com) has funded the SAR imagery processing as well as the geological reconstruction presented in the paper. The authors gratefully acknowledge TeleRilevamento Europa (TRE) for having processed the SAR data. Boreholes data derive from the CNR IGAG database of UrbiSIT Project, funded by the Italian Department of Civil Protection (DPC). Federico Di Traglia is supported by a post-

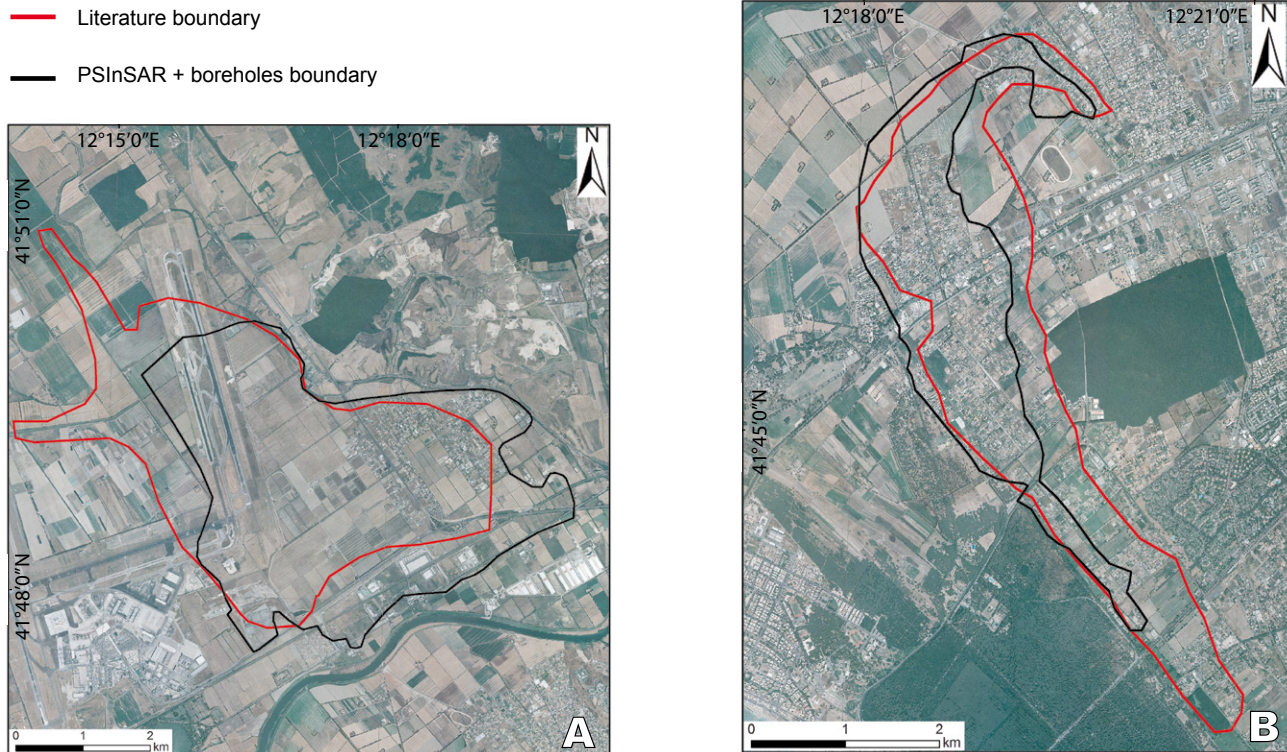


FIGURE 12. 2D reconstruction of the extension of the peat layer in A) Maccarese and B) Ostia ponds. Pond limits (black polyline) determined using PSInSAR data and boreholes; in red pond boundary from the literature (Giraudi, 2011 for Maccarese pond and Geolithologic map of Rome municipality for Ostia pond).

doc fellowship founded by the Regione Toscana (UNIFI-FSE) under the project “Space-born and ground-based SAR techniques for the evaluation of natural hazard” (RadSafe - UNIFI-4) in the framework of the research agreement between DST-UNIFI, DST-UNIFI and Ellegi s.r.l. - Lisalab.

REFERENCES

- Amenduni, G., 1884. Sulle opere di bonificazione della plaga litoranea dell’Agro Romano che comprende le paludi e gli stagni di Ostia, Porto, Maccarese e delle terre vallive di Stracciaccapa, Baccano, Pantano e Lago dei Tartari. Relazione del progetto generale 15/7/1880. Roma, Ministero dei Lavori Pubblici, Ed. E. Botta, 1-36.
- Amorosi, A., Milli, S., 2001. Late Quaternary depositional architecture of Po and Tevere river deltas (Italy) and worldwide comparison with coeval deltaic successions. *Sedimentary Geology*, 144, 357-375.
- Bellotti, P., Biagi, P.F., Tortora, P., Valeri, P., 1987. Il delta del Tevere: caratteri morfologici e sedimentologici della piana deltizia. *Giornale di Geologia*, 49, 89-99.
- Bellotti, P., Milli, S., Tortora, P., Valeri, P., 1995. Physical stratigraphy and sedimentology of the late Pleistocene-Holocene Tiber Delta depositional sequence. *Sedimentology*, 42, 617-634.
- Bellotti, P., Calderoni, G., Carboni, M.G., Di Bella, L., Tortora, P., Valeri, P., Zernitskaya, V., 2007. Late Quaternary landscape evolution of the Tiber River delta plain (Central Italy): new evidence from pollen data, biostratigraphy and ¹⁴C dating. *Eitschrift für Geomorphologie*, 51, 505-534.
- Bellotti, P., Calderoni, G., Di Rita, F., D’Orefice, M., D’Amico, C., Esu, D., Magri, D., Preite Martinez, M., Tortora, P., Valeri, P., 2011. The Tiber River delta plain (central Italy): Coastal evolution and implications for the ancient Ostia Roman settlement. *The Holocene*, 21(7), 1105-1116.
- Belluomini, G., Iuzzolini, P., Manfra, L., Mortari, R., Zalaffi, M., 1986. Evoluzione recente del delta del Tevere. *Geologica Roma*, 25, 213-234.
- Bianchini, S., Cigna, F., Del Ventisette, C., Moretti, S., Casagli, N., 2012. Detecting and monitoring landslide phenomena with TerraSAR-X persistent scatterers data: the Gimigliano case study in Calabria Region (Italy). *International Geoscience and Remote Sensing Symposium (IGARSS)*, 982-985.
- Bianchini, S., Cigna, F., Del Ventisette, C., Moretti, S., Casagli, N., 2013. Monitoring landslide-induced displacements with TerraSAR-X persistent scatterer interferometry (PSI): Gimigliano case study in Calabria Region (Italy). *International Journal of Geosciences*, 4, 1467-1482.

- Bürgmann, R., Hilley, G.E., Ferretti, A., 2006. Resolving vertical tectonics in the San Francisco Bay Area from Permanent Scatterer InSAR and GPS Analysis. *Geology*, 34, 221-224.
- Canuti, P., Casagli, N., Farina, P., Ferretti, A., Marks, F., Menduni, G., 2005. Land subsidence in the Arno river basin studied through SAR Interferometry. Shanghai, China, Proceedings of SISOLS 2005, 7th International Symposium on Land Subsidence, 23–28 October 2005, 1, 407-416.
- Capelli, G., Mazza, R., Papiccio, C., 2007. Intrusione salina nel Delta del Fiume Tevere. *Geologia, idrologia e idrogeologia del settore romano della piana costiera. Giornale di Geologia Applicata*, 5, 13-28.
- Ciampalini, A., Cigna, F., Del Ventisette, C., Moretti, S., Liguori, V., Casagli, N., 2012. Integrated geomorphological mapping in the north-western sector of Agrigento (Italy). *Journal of Maps*, 8(2), 136-145.
- Cigna, F., Del Ventisette, C., Liguori, V., Casagli, N., 2010. InSAR time-series analysis for management and mitigation of geological risk in urban area. *IEEE International Symposium on Geoscience and Remote Sensing IGARSS*, 1924-1927.
- Cigna, F., Del Ventisette, C., Liguori, V., Casagli, N., 2011. Advanced radar-interpretation of InSAR time series for mapping and characterization of geological processes. *Natural Hazard and Earth System Sciences*, 11, 865-881. DOI:10.5194/nhess-11-865-2011.
- Cigna, F., Del Ventisette, C., Gigli, G., Menna, F., Agili, F., Liguori, V., Casagli, N., 2012. Ground instability in the old town of Agrigento (Italy) depicted by on-site investigations and Persistent Scatterers data. *Natural Hazards and Earth System Science*, 12, 3589-3603.
- Cigna, F., Liguori, V., Del Ventisette, C., Casagli, N., 2013. Landslide impact on Agrigento's cathedral imaged with radar interferometry. *Landslide Sciences and practise: Risk Assessment, management and mitigation*, 6, 475-481.
- Colesanti, C., Ferretti, A., Prati, C., Rocca, F., 2003. Monitoring landslides and tectonic motions with the Permanent Scatterers Technique. *Engineering Geology*, 68, 3-14.
- Del Ventisette, C., Ciampalini, A., Calò, F., Manunta, M., Paglia, L., Reichenbach, P., Colombo, D., Mora, O., Strozzi, T., Garcia, I., Mateos, R., Herrera, G., Füsü, B., Graniczny, M., Przylucka, M., Retzo, H., Moretti, S., Casagli, N., Guzzetti, F., 2013. Exploitation of large archives of ERS and ENVISAT C-Band SAR data to characterize ground deformation. *Remote Sensing*, 5(8), 3896-3917.
- Del Ventisette, C., Righini, G., Moretti, S., Casagli, N., 2014. Multitemporal landslides inventory map updating using spaceborne SAR analysis. *International Journal of Applied Earth Observation and Geoinformation*, 30, 238-246.
- Farina, P., Colombo, D., Fumagalli, A., Marks, F., Moretti, S., 2006. Permanent Scatterers for landslide investigations: outcomes from the ESA-SLAM project. *Engineering Geology*, 88, 200-217.
- Ferretti, A., Prati, C., Rocca, F., 2000. Nonlinear subsidence rate estimation using Permanent Scatterers in differential SAR interferometry. *IEEE Transactions on Geoscience and Remote Sensing*, 38(5), 2202-2212.
- Ferretti, A., Prati, C., Rocca, F., 2001. Permanent Scatterers in SAR interferometry. *IEEE Transactions on Geoscience and Remote Sensing*, 39(1), 8-20.
- Giraudi, C., 2004. Evoluzione tardo-olocenica del delta del Tevere. *Il Quaternario*, 17, 477-492.
- Giraudi, C., 2011. The sediments of the “Stagno di Maccarese” marsh (Tiber River delta, central Italy): A late-Holocene record of natural and human-induced environmental changes. *The Holocene*, 21(8), 1233-1243.
- Hilley, G.E., Burgmann, R., Ferretti, A., Novali, F., Rocca, F., 2004. Dynamics of slow-moving landslides from permanent scatterer analysis. *Science*, 304 (5679), 1952-1955.
- Kampes, B.M., 2006. *Radar Interferometry Persistent Scatterer Technique*. Dordrecht, The Netherlands, Springer, 227pp.
- Massironi, M., Zampieri, D., Bianchi, M., Schiavo, A., Franceschini, A., 2009. Use of PSInSAR™ data to infer active tectonics: Clues on the differential uplift across the Giudicarie belt (Central-Eastern Alps, Italy). *Tectonophysics*, 476, 297-303.
- Massonnet, D., Feigl, K.L., 1998. Radar interferometry and its application to changes in the earth's surface. *Reviews of Geophysics*, 36 (4), 441-500.
- Milli, S., D'Ambrogi, C., Bellotti, P., Calderoni, G., Carboni, M.G., Celant, A., Di Bella, L., Di Rita, F., Frezza, V., Magri, D., Pichezzi, R.M., Ricci, V., 2013. The transition from wave-dominated estuary to wave-dominated delta: The Late Quaternary stratigraphic architecture of Tiber River deltaic succession (Italy). *Sedimentary Geology*, 284-285, 159-180.
- Osmanoglu, B., Dixon, T.H., Wdowinski, S., Cabral-Cano, E., Jiang, Y., 2011. Mexico City subsidence observed with Persistent Scatterer InSAR. *International Journal of Applied Earth Observation and Geoinformation*, 13(1), 1-12.
- Perrone, G., Morelli, M., Piana, F., Fioraso, G., Nicolò, G., Mallen, L., Cadoppi, P., Balestro, G., Tallone, S., 2013. Current tectonic activity and differential uplift along the Cottian Alps/Po Plain boundary (NW Italy) as derived by PS-InSAR data. *Journal of Geodynamics*, 66, 65-78.
- Raspa, G., Moscatelli, M., Stigliano, F.P., Patera, A., Folle, D., Vallone, R., Mancini, M., Cavinato, G.P., Milli, S., Costa, J.F.C.L., 2008. Geotechnical characterization of the upper Pleistocene–Holocene alluvial deposits of Roma (Italy) by means of multivariate geostatistics: crossvalidation results. *Engineering Geology*, 101, 251-268.
- Salvi, S., Atzori, S., Tolomei, C., Allievi, J., Ferretti, A., Rocca, F., Prati, C., Stramondo, S., Feuillet, N., 2004. Inflation rate of the Colli Albani volcanic complex retrieved by the permanent scatterers SAR interferometry technique. *Geophysical Research Letters*, 31(21), L12606.

Stramondo, S., Bozzano, F., Marra, F., Wegmuller, U., Cinti, F.R., Moro, M., Saroli, M. 2008. Subsidence induced by urbanization in the city of Rome detected by advanced InSAR technique and geotechnical investigations. *Remote Sensing Environment*, 112, 3160-3172.

Tizzani, P., Berardino, P., Casu, F., Euillades, P., Manzo, M., Ricciardi, G.P., Zeni, G., Lanari, R., 2007. Surface deformation of Long Valley caldera and Mono Basin, California, investigated with the SBAS-InSAR approach. *Remote Sensing Environment*, 108, 277-289.

Tofani, V., Del Ventisette, C., Moretti, S., Casagli, N., 2014. Integration of remote sensing techniques for intensity zonation within a landslide area: a case study in the Northern Apennines, Italy. *Remote Sensing*, 6(2), 907-924.

Manuscript received May 2014;
revision accepted March 2015;
published Online November 2015.

ELECTRONIC APPENDIX I

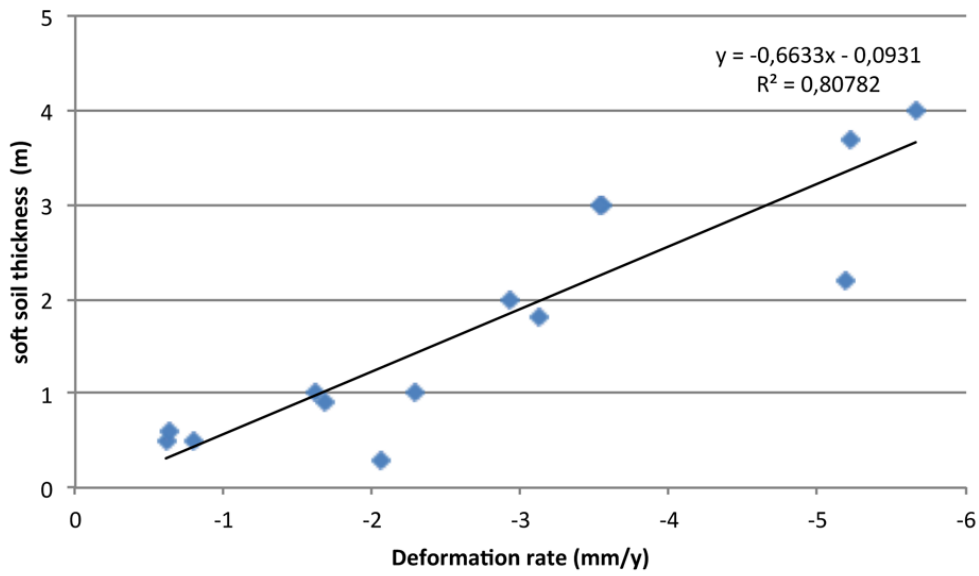


FIGURE I. Correlation diagram between PS velocity and soft soil thickness in Ostia area.

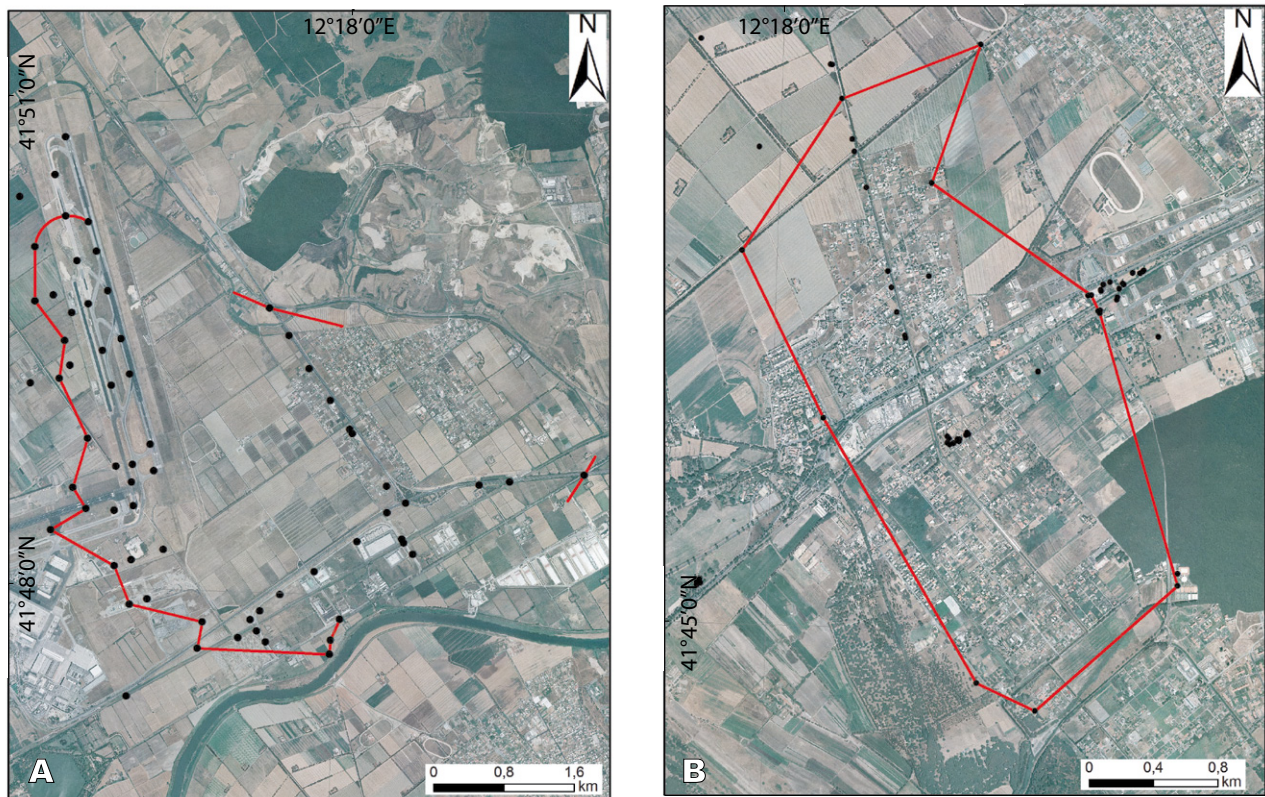


FIGURE II. Contour reconstruction of the peat layer in the two analyzed areas with the boreholes information; A) Maccarese, B) Ostia.

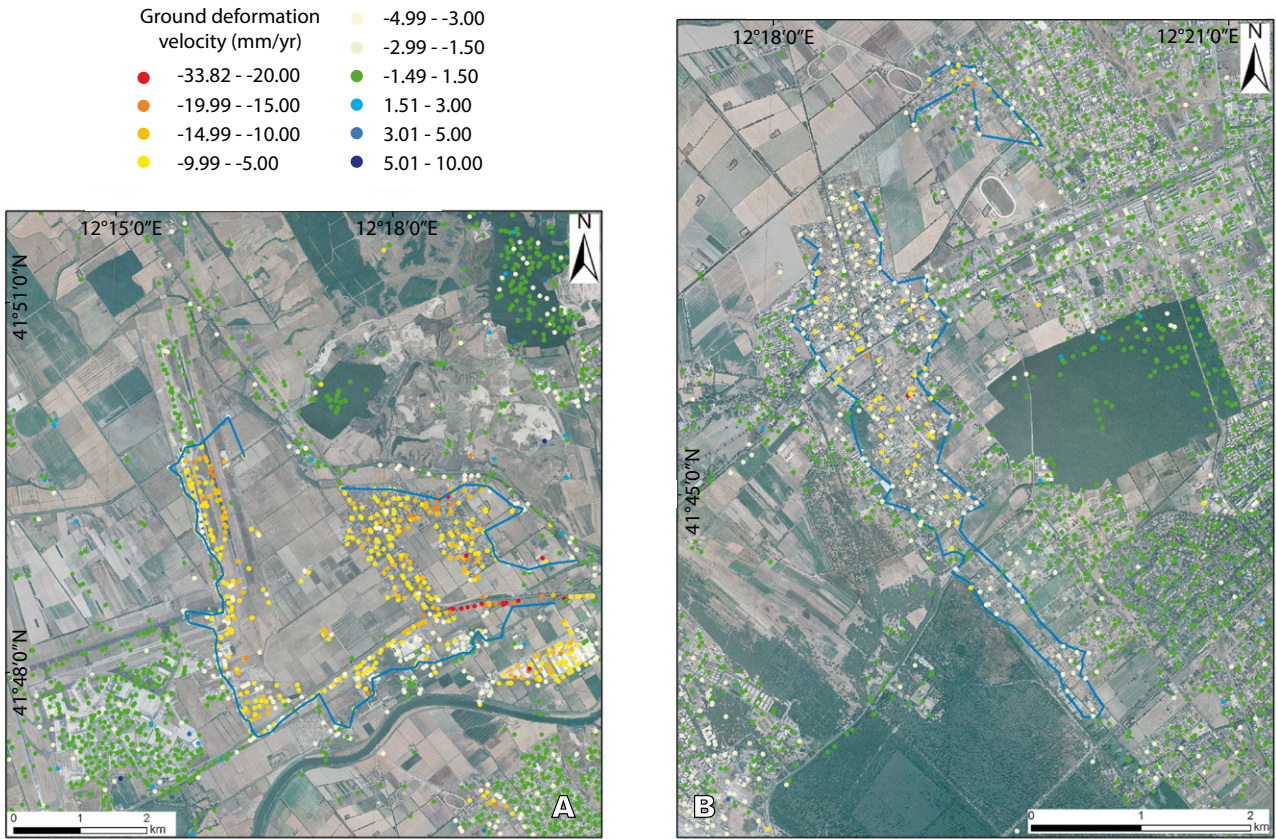


FIGURE III. Contour reconstruction of the peat layer with PSInSar data; A) Maccarese, B) Ostia.